Supporting Information

Expression-Enhanced Fluorescent Proteins Based on Enhanced Green Fluorescent Protein for Super-Resolution Microscopy

Sam Duwé, Elke De Zitter, Vincent Gielen, Benjamien Moeyaert, Wim Vandenberg, Tim Grotjohann, Koen Clays, Stefan Jakobs, Luc Van Meervelt, Peter Dedecker

DISCUSSION OF SUPERFOLDER MUTATIONS

The superfolder mutations (S30R, Y39N, N105T/Y and I171V) were structurally highly similar in rsGreen0.7 compared to sfGFP. Arginine 30 has the same conformation in rsGreen0.7 (off-state) as in sfGFP, resulting in a similar electrostatic network stabilizing β-strands 1, 2, 5 and 6. This network is not present in EGFP. It adopts a different conformation in the on-state rsGreen0.7, but can still form a stabilizing network through an additional water molecule (Figure S19, supporting information). Compared to sfGFP, both the on- and the off-state structure of rsGreen0.7 reveal a different conformation for Asn39. Whereas this asparagine in sfGFP forms a direct interaction with aspartate 36, tightening the loop between β-strands 2 and 3, the different conformation in rsGreen0.7 allows a hydrogen-bonding network to the sidechain of aspartate 36 through a water molecule (Figure S20, supporting information). Around residue 105 many residues display multiple conformations in the crystal structures indicating a high degree of flexibility. Therefore, the increased stability may be caused by the high β-sheet propensity of threonine (rsGreen0.7) and tyrosine (sfGFP) compared to arginine (EGFP, rsEGFP). The I171V mutation in rsGreen0.7 adopts the same conformation as seen in sfGFP and most likely causes side chain stabilization through nonpolar interactions. As for the cycle-3 mutations, F99S and M153T, no structural rearrangements could be detected in the crystal structures in relation to EGFP and sfGFP. Both mutations likely act by reducing the overall hydrophobicity of the proteins.[1] Mutation S72A is well known to improve the chromophore maturation and folding kinetics, although the mechanism remains unclear.

Although no crystal structures of other rsGreens are available at present, we can use the rsGreen0.7 crystal structures to speculate about the role of the other introduced mutations. The mutation of leucine 44, a buried residue at the back of the chromophore, to methionine improves

the photoswitching while slightly reducing the brightness (rsGreen0.9). While multiple conformations of leucine 44 are observed in the EGFP structure (4EUL)[2] indicating flexibility, our structures and the sfGFP structures (2B3P, 4LQT)[3,4] reveal only a single conformation, which might be due to the increased rigidity or stability introduced by superfolder mutations. Because methionine has more degrees of freedom than leucine, we speculate that it enhances the flexibility of the chromophore environment, allowing efficient photoswitching.[5] K101E and K162R are both located near loop regions, facing outward. The additional polar interactions could stabilize otherwise flexible regions of the FP leading to an increase in the overall structural stability. Interestingly, the K101E mutation was also identified in an intermediate product during the evolution towards superfast GFP, but was not retained in the final version.[6] The H169L mutation affects both brightness, which is increased, and photoswitching contrast, which is decreased. Furthermore, it is likely to be the cause of the pKa difference between rsGreen0.8 (pKa = 6.7) and rsGreen0.9 (pKa = 5.7), due to its proximity to the chromophore and residue 145. Mutation A227S, leading to increased brightness, introduces the possibility for polar interactions and can have a large impact on the otherwise more flexible C-terminal region. The final rsGreen1 mutation, N149D is situated near the chromophore *p*-hydroxyphenyl moiety and several other residues that influence photoswitching, such as histidine 148.[7] Therefore, an effect on the brightness and photochromism was to be expected, although the reason or mechanism remains unclear as its side chain points outwards the β-can.

MATERIALS AND METHODS

Supporting Method 1: Screening, brightness analysis & switching analysis

Library screening for brightness and photoswitching behavior was performed on a colony imaging system adapted from Mizuno and coworkers.[8] The system consists of a 300 W xenon lamp (MAX-302, Asahi Spectra) with a motorized filter exchanger, a cooled EMCCD camera (Cascade 512B, Photometrics) equipped with a c-mount lens (Fujinon TV 1:1.4/16, Fuji Photo Optical Co.) and a motorized filter wheel (FW102C, Thorlabs) All components are driven by a home written routine in IgorPro (Wavemetrics). The light from the ASAHI lamp was passed through a 480/40 bandpass filter for both excitation and off-switching. On switching light was achieved by passing the light through a 400/30 bandpass filter. Images were recorded by the EMCCD camera through a 530/40 bandpass filter. Imaging parameters such as acquisition time (0.1-1 s) and illumination power (0-100%) were adjusted to make optimal use of the available dynamic range. Single images are sufficient for brightness analysis, while photoswitching was screened for by time-lapse imaging of the colonies under differing illumination conditions. A typical photoswitching screen consisted of 60-150 s illumination through the 400/30 bandpass filter at 30% of maximum power to induce on-switching, followed by 20 min off-switching (illumination through the 480/40 bandpass filter at full power) and 15 min on-switching (400/30 bandpass filter at 30% of maximum power). Images were recorded every 30 s using excitation light passing through the 480/40 bandpass filter.

During directed mutagenesis screening, 2-3 brightest colonies were selected, picked and cultured, miniprepped and transformed in JM109(DE3) *E. coli* cells. Multiple clones were plated in distinct regions of the same bacterial growth plate, which also included a region with colonies

expressing the template protein. Clones brighter than the template were sent for sequencing (LGC Genomics) and used as a template in a subsequent mutagenesis approach. Only clones that exhibited obvious reversible photoswitching behavior were considered for characterization and further mutagenesis. StEP mutagenesis libraries were screened similarly, but a larger amount (5-15) of bright colonies was primarily selected for comparative screening.

Libraries generated by random mutagenesis were either screened or completely pooled and used as a template for subsequent random mutagenesis. When screened, up to 100 bright colonies from a single plate were picked, pooled, grown, miniprepped and used for subsequent mutagenesis. The brightest clones (~5) were cultured separately and used for comparative screening.

To identify mutants with increased switching behavior, a ratio image of the on-state, before illumination through the 480/40 filter, over the off-state, after illumination through the 480/40 filter, was calculated. The resulting image allowed for the fast and easy identification of good switchers, displaying higher contrast values.

Supporting Method 2: Expression and purification

Expression was performed in a JM109(DE3) (Promega) *E. coli* strain relying on leak expression of the T7 promotor controlling the inserted gene. A fresh colony (15-24 hours after transformation) was used to inoculate 200-300 mL LB (Luria Bertani) medium supplemented with 100 µg/mL ampicillin and grown for 48-72 hours at 21°C with constant shaking (200-250 rpm.). Cells were spinned down for 15 minutes at 5000 rpm and 4°C and the cell pellet was resuspended in ice-cold PBS supplemented with protease inhibitor (cOmplete mini, Roche). The *E. coli* cells were lysed using a french pressure cell and the cellular debris was spinned down for

10 minutes at 8000 rpm and 4°C. The supernatant was incubated with Ni-NTA agarose resin (Qiagen) and the recombinant FPs were allowed to bind to the resin for approximately 1 hour at 4°C under constant mixing. The Ni-NTA agarose was allowed to pack onto polypropylene 5 mL columns (Thermo scientific) and washed with excess TN buffer (100 mM Tris-HCl, 300 mM NaCl, pH 7.4). Elution of the proteins was done using TN buffer supplemented with 200 mM imidazole. Buffer exchange using PD-10 desalting columns (GE Healthcare) was used, eluting the proteins in regular TN buffer or PBS. Protein solutions were stably stored at 4°C for the duration of the experiments.

Supporting Method 3: Eukaryotic cell culture

For flow cytometry and microscopy experiments, HeLa cells and HEK293T cells were cultured in DMEM supplemented with 10% (v/v) FBS, 1% (v/v) glutaMAX^{TM} and 0.1% (v/v) gentamicin (all Gibco) and subcultured every 3-4 days. Before transfection, 250000 - 500000 HeLa cells were seeded in 35 mm glass bottom dishes (MatTek) or a 6 well plate (CELLSTAR, Greiner) and incubated overnight. Cells were transfected using the calcium phosphate method. Briefly, 32 mL $CaCl_2$ (2 M) was thoroughly mixed with 5 µg plasmid DNA in 218 µL dH_2O to a total volume of 250 µL. This DNA mixture was added dropwise to 250 µL 2x HBS (50 mM HEPES, 280 mM NaCl, 1.5 mM Na_2HPO_4 at pH 7.05-7.06, filter sterilized) and immediately added to the medium on top of the cells. Care was taken not to disturb the DNA complexes. Cells were washed twice with PBS (pH 7.4) after 8-12 hours and supplied with fresh growth medium.

For Flow cytometry analysis, equal amounts of plasmid DNA were used for each transfection. Control experiments were performed by measuring untransfected cells and cells transfected with pcDNA3 (negative controls) and pcDNA3::EGFP (positive control). 24 hours post transfection;

the cells were washed twice with PBS and loosened by covering the cells with a mixture of trypsin in PBS and placing the cells at 37°C for 2-5 min. The cells were loosened further by gentle tapping and the trypsin was deactivated by the addition of DMEM supplemented with 10% (v/v) FBS. The entire cell suspension was centrifuged at 400 g for 5 minutes, the supernatant was removed and the cell pellet was gently resuspended in 1mL fresh HBSS (8 g/L NaCl, 400 mg/L KCl, 1 g/L glucose, 350 mg/L $NaHCO_3$, 60 mg/L KH_2PO_4 and 47.86 mg/L Na_2HPO_4). This process was repeated once more and cells were transported to the KU Leuven FACS Core. 20 minutes prior to the cytometry experiment, 10 µL of a 7-AAD solution (1 mg 7-AAD in 50 µL DMSO and 950 µL PBS) was added to the cell suspension and incubated in the dark. All manipulations were performed at room temperature.

Prior to pcSOFI imaging and widefield microscopy (24-48 hours after transfection), cells were washed 3x with preheated PBS (Gibco) and 2 mL HBSS (Gibco) was added to allow cell survival at conditions without 5% CO_2.

For RESOLFT imaging, HeLa cells were grown at 37 °C and 5% CO2 in DMEM (Invitrogen, Carlsbad, CA) containing 5% FCS (PAA, Pasching, Austria), 100 units per ml streptomycin, 100 µg/ml penicillin (all Biochrom, Berlin, Germany), and 1 mM pyruvate (Sigma, St. Louis, USA). For transfection, cells were seeded on cover glasses in 6-well plates. Transfection was performed with Turbofect (Life technologies, Carlsbad, CA, USA) according to the manufacturer's instructions. RESOLFT images were recorded one day after transfection.

Supporting Method 4: X-ray data collection, analysis and refinement

X-ray diffraction data of rsGreen0.7 in its green-on state was collected under a nitrogen cryostream of 100 K, using a wavelength of 1.00 Å (12.4 keV) and a PILATUS detector at the XRD1 beamline of Elettra, Italy. Data collection of rsGreen0.7 green-off was performed at the PROXIMA 1 beamline at Soleil, France. Also here, a cold nitrogen stream of 100 K and a PILATUS detector were used, but a wavelength of 0.8856 Å (14.0 keV) was used.

The data of both the rsGreen0.7 on- and off state was indexed and integrated using XDS v. January 10, 2014[9] and scaled and merged using Phenix.reflection file editor[10]. The structures were solved by molecular replacement using Phaser v.2.5.6[11]. The coordinates of superfolder GFP (PDB ID: 2B3P) and rsGreen0.7 in the on-state were used as phasing models in solving the structure of the green-on state and the off-state, respectively. The likelihood-based refinement was carried out using Phenix.refine v.1.9[12]. The subsequent refinement cycles consisted of three macro-cycles of bulk-solvent and anisotropic scaling, individual coordinate and occupancy refinement.

After the first refinement cycle, the chromophores and mutated residues were modelled in the difference map, using Coot v.0.7.2[13]. Water molecules were included in the model if they were within hydrogen bonding distance (2.2 – 3.5 Å) to chemically reasonable groups, appeared in mFo-DFc maps contoured at 3.0 σ, and had a B-factor less than 80 $Å^2$. Riding hydrogen atoms were added to both structures. B-factors were anisotropically refined for non-hydrogen protein atoms in residues with a single conformation. The other atoms and water molecules have isotropically refined B-factors. Standard dictionary files were used for the amino acid residues, with additional dictionary files created by eLBOW[14] for the chromophore.

The structure of rsGreen0.7 in its green-off state also contains electron density for the on-state structure. Therefore, at position 203, 204, 205, 148 and the chromophore (residues with big differences between the on- and off-state), on-state residues were modeled as alternative conformations named B. Their occupancies were linked to each other and got an occupancy factor of 42%. To differentiate between these "on-state" residues and alternative configurations in the off-state, the latter were modeled as alternative conformations named C.

The data collection and refinement statistics can be found in Table S4 (supporting information). The structures of rsGreen0.7 green-on and green-off were deposited in the PDB with codes 4XOW and 4XOV, respectively. Images were created using Pymol (www.pymol.com).

Table S1: List of directed mutations tested in rsEGFP during the development of rsGreen0.7.

Mutation	Present in rsGreenX	References
Ser30Arg	Yes	3,15
Tyr39Asn	Yes	3,15
Val68Leu	No	6,16,17
Ser72Ala	Yes	6,16–22
Phe99Ser	Yes	1,3,15,23
Asn105Thr	No	3,15
Asn105Tyr	Yes	6
Glu124Val	No	6
Tyr145Phe	Yes*	3,6,15,18,22
Ser147Pro	No	24,25
Asn149Lys	No	18–20
Met153Thr	Yes	1,3,15,17,21,23
Ile167Thr	No	18–21,26
Ile171Val	Yes	3,15
Ser175Gly	No	17,22,26
Thr203His	No	15,18,27

Mutations that improved the in colony brightness of the ferritin-rsEGFP construct were kept in the final variant. Mutations that did not cause a visible improvement in brightness were discarded. * not present in rsGreen0.7b

Table S2: Renaturation and theoretical maturation of EGFP, rsEGFP, rsEGFP2, rsGreen0.7,

	EGFP	rsEGFP		rsGreen					
		1	2	0.7	0.7b	0.8	0.9	1	F
Maturation (*E. coli* brightness / molecular brightness)	1.0	0.2	1.8	5.0	2.4	6.4	4.2	5.1	8.0
Maturation (HEK293T brightness / molecular brightness)	1.0	0.2	0.4	1.0	ND	1.0	0.4	0.5	0.7
Renaturation rate 1 (10^{-2} s^{-1})	3.4	3.6	8.1	4.5	4.9	4.1	6.0	4.7	4.4
Renaturation rate 2 (10^{-3} s^{-1})	4.5	5.1	5.5	6.5	6.8	7.1	9.1	8.2	7.6

Renaturation rate 1 and 2 are determined by the double-exponential fit of the renaturation data and used to calculate the weighted average renaturation rate listed in Table 1.
rsGreen0.7b, rsGreen0.8, rsGreen0.9, rsGreen1 and rsGreenF.

Table S3: List of primers.

name	sequence	role
(rs)EGFP BamHI FWD	5'-GCGGGATCCGATGGTGAGCAAGGGCGAG	pRSETb-FP / pcDNA3-Lyn-FP / pcDNA3-DAKAP-FP / pcDNA3-FP
(rs)EGFP EcoRI REV*	5'-GCGAATTCTTACTTGTACAGCTCGTC	
(rs)EGFP AGSG FWD	5'-GCGGTACCGCTGGTTCTGGCGAATTCATGGTGAGCAAGGGCGAG	
(rs)EGFP AGSAAGSG FWD	5'-GCGGTACCGCTGGCTCCGCTGCTGGTTCTGGCGAATTCATGGTG	
(rs)EGFP HindIII REV*	5'-GCAAGCTTTTACTTGTACAGCTCGTC	pRSETb-Ferritin-FP
Ferritin BamHI FWD	5'-GCGGATCCGATGGACTCACAGGTGCGCCAG	
Ferritin KpnI REV	5'-GCGGTACCAGAGGATTCCCCCATGGTG	
(rs)EGFP HindIII FWD	5'-GCGAAGCTTGCCACCATGGTGAGCAAGGGCGAGGAGC	pcDNA3-FP-Tubulin
(rs)EGFP BamHI REV	5'-GCGGGATCCCTTGTACAGCTCGTCCATGC	
(rs)EGFP AgeI FWD	5'-TCCACCGGTCGCCACCATGGTGAGCAAGGGCGAGGAGCTGTTC	prsGreenF-vimentin
(rs)EGFP NotI REV	5'-GTCGCGGCCGCTACTTGTACAGCTCGTCCATGCCGAGAG	
rsEGFP-S30R	5'-CAAGTTCAGCGTGCGCGGCGAGGGCGAG	QC primers
rsEGFP-Y39N	5'-GGGCGATGCCACCAACGGCAAGCTGAC	
rsGreen0.8-L44M	5'-CAACGGCAAGCTGACCATGAAGTTCATCTGCAC	
rsEGFP-V68L	5'-CCCTGACCTACGGCTTGCTGTGCTTCAGC	
rsEGFP-S72A	5'-CGTGCTGTGCTTCGCCCGCTACCCCGAC	
rsEGFP-F99S	5'-CAGGAGCGCACCATCAGCTTCAAGGACGACGG	
rsGreen0.8-K101E	5'-CGCACCATCAGCTTCGAGGACGACGGCTATT	
rsEGFP-N105T	5'-CAAGGACGACGGCACCTACAAGACCCGCG	
rsEGFP-T105Y	5'-CTTCAAGGACGACGGCTATTACAAGACCCGCGCCG	
rsEGFP-E124V	5'-GGTGAACCGCATCGTGCTGAAGGGCATCG	
rsEGFP-Y145F	5'-AAGCTGGAGTACAACTTCAACAGCCACAACGCC	
rsGreen0.7-F145Y	5'-CACAAGCTGGAGTACAACTATAACAGCCACAACGCCTATA	
rsEGFP-S147P	5'-GCTGGAGTACAACTTCAACCCCCACAACGCCTATATCACG	
rsEGFP-N149K	5'-TACAACTTCAACAGCCACAAGGCCTATATCACGG	
rsEGFP-M153T	5'-ACAGCCACAACGCCTATATCACGGCCGACAAGC	
rsEGFP-I167T	5'-CGGCATCAAGTCTAACTTCAAGACCCGCCACAACGT	
rsGreen0.8-H169L	5'-CTTCAAGATCCGCCTCAACGTCGAGGACG	
rsEGFP-I171V	5'-GATCCGCCACAACGTCGAGGACGGCAG	
rsEGFP-S175G	5'-GTCGAGGACGGCGGCGTGCAGCTCG	
rsEGFP-T203H	5'-CGACAACCACTACCTGAGCCACCAGAATAAGCTGAGCAAA	

Table S4: Crystallographic data collection and refinement statistics.

	rsGreen0.7 green-on	rsGreen0.7 green-off
PDB ID	4XOW	4XOV
Space group	$P2_12_12_1$	$P2_12_12_1$
Unit cell parameters		
a, b, c (Å)	31.76 61.60 105.70	31.99 61.31 105.74
Resolution range (Å)	40.11 – 1.25 (1.29 – 1.25)*	40.04 – 1.20 (1.24 – 1.20)
R_{merge} (%)	8.7 (73.1)	17.0 (65.6)
R_{meas} (%)	9.5 (79.7)	18.3 (70.7)
$R_{p.i.m.}$ (%)	3.8 (31.3)	6.8 (26.2)
$CC^{1/2}$ (%)	99.9 (79.3)	98.2 (75.6)
$\langle I/\sigma(I)\rangle$	13.4 (2.6)	6.8 (2.0)
No. of reflections	364035 (36386)	477387 (46293)
No. of unique reflections	58259 (5745)	66033 (6516)
Multiplicity	6.2 (6.3)	7.2 (7.1)
Completeness (%)	99.7 (100.0)	100.0 (100.0)
V_M (Å^3/Da)	1.99	2.07
Solvent content (%)	38.2	40.7
Molecules per asymmetric unit	1	1
Mosaicity (°)	0.27	0.04
R_{work}/R_{free} § (%)	14.07/16.49	14.31/16.84
RMSD from ideal		
Bond lengths (Å)	0.008	0.009
Bond angles (°)	1.339	1.349
No. of atoms		
Protein	3835	4145
Water	365	291
Average isotropic B-factors (Å^2)		
Main chain	9.6	17.2
Side chain	13.9	23.0
Water molecules	27.8	32.0
Ramachandranplot # (%)		
Residues in favored regions	98.7	98.4
Residues in allowed regions	1.3	1.6
Outliers	0.0	0.0
Rotamer# outliers (%)	0.5	0.9

* Values in parentheses are for the highest resolution shell.

§R_{free} is calculated using a random 5% of data excluded from the refinement.

#Ramachandran and rotamer analysis was carried out using Molprobity[28].

Table S5: Interactions of the *p*-hydroxyphenyl oxygen atom in the on- and off-state of reversibly photoswitchable fluorescent proteins.

Protein	On-state		Off-state	
Dronpa[29,30]	2IE2	Ser142, H_2O	2POX	H_2O
pcDronpa[31]	4HQ8	Ser142	4HQ9	Glu144, H_2O
IrisFP[32]	2VVH	Ser142, H_2O	2VVI	Glu144, H_2O
rsTagRFP[33]	3U8C (*trans*)	H_2O	3U8A	H_2O
Padron[34]	3ZUJ	Ser142	3ZUF	Gly144, Tyr159, H_2O
Dreiklang[35]	3ST4	H_2O	3ST3	H_2O
asFP595[36]	2A52	H_2O	2A50	Ser158, H_2O
mTFP0.7[37]	2OTB	His163, SerS46, H_2O	2OTE	Glu148, H_2O

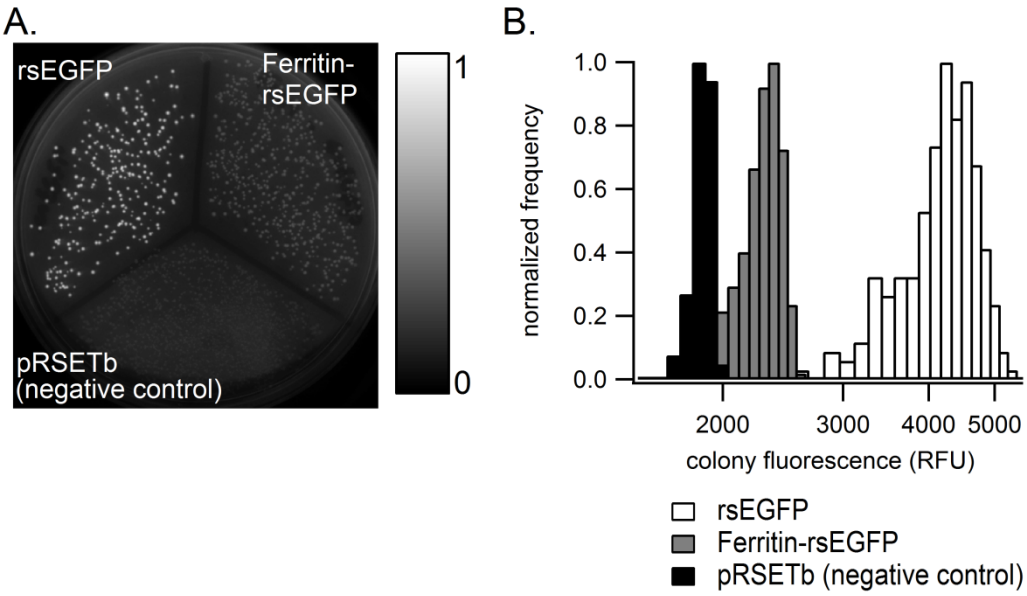

Figure S1: (A.) Comparison of *E. coli* colonies expressing rsEGFP, Ferritin-rsEGFP and no FP from pRSETb. (B.) Histogram of colony brightness of the bacterial plate depicted in (A.). The reduction in fluorescence when rsEGFP is fused to ferritin is apparent.

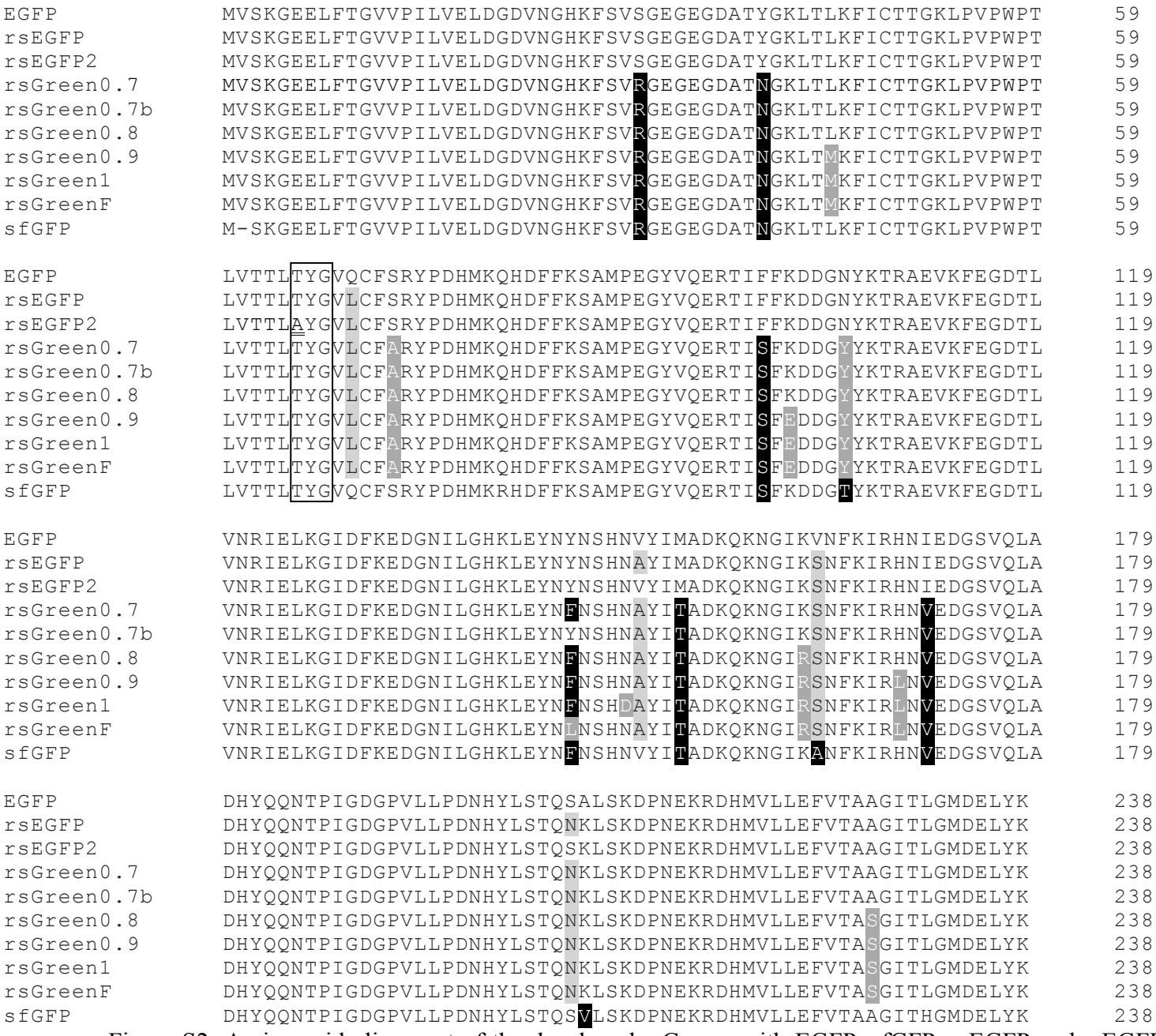

Figure S2: Amino acid alignment of the developed rsGreens with EGFP, sfGFP, rsEGFP and rsEGFP2. The chromophore is indicated by the boxed region with the rsEGFP2 mutation underlined. Mutations introduced during the development of rsEGFP are indicated as black letters highlighted in grey. Mutations introduced into rsEGFP during the development of rsGreens are represented by white letters. sfGFP mutations highlighted in black, mutations based on other FPs and found by random mutagenesis highlighted in grey.

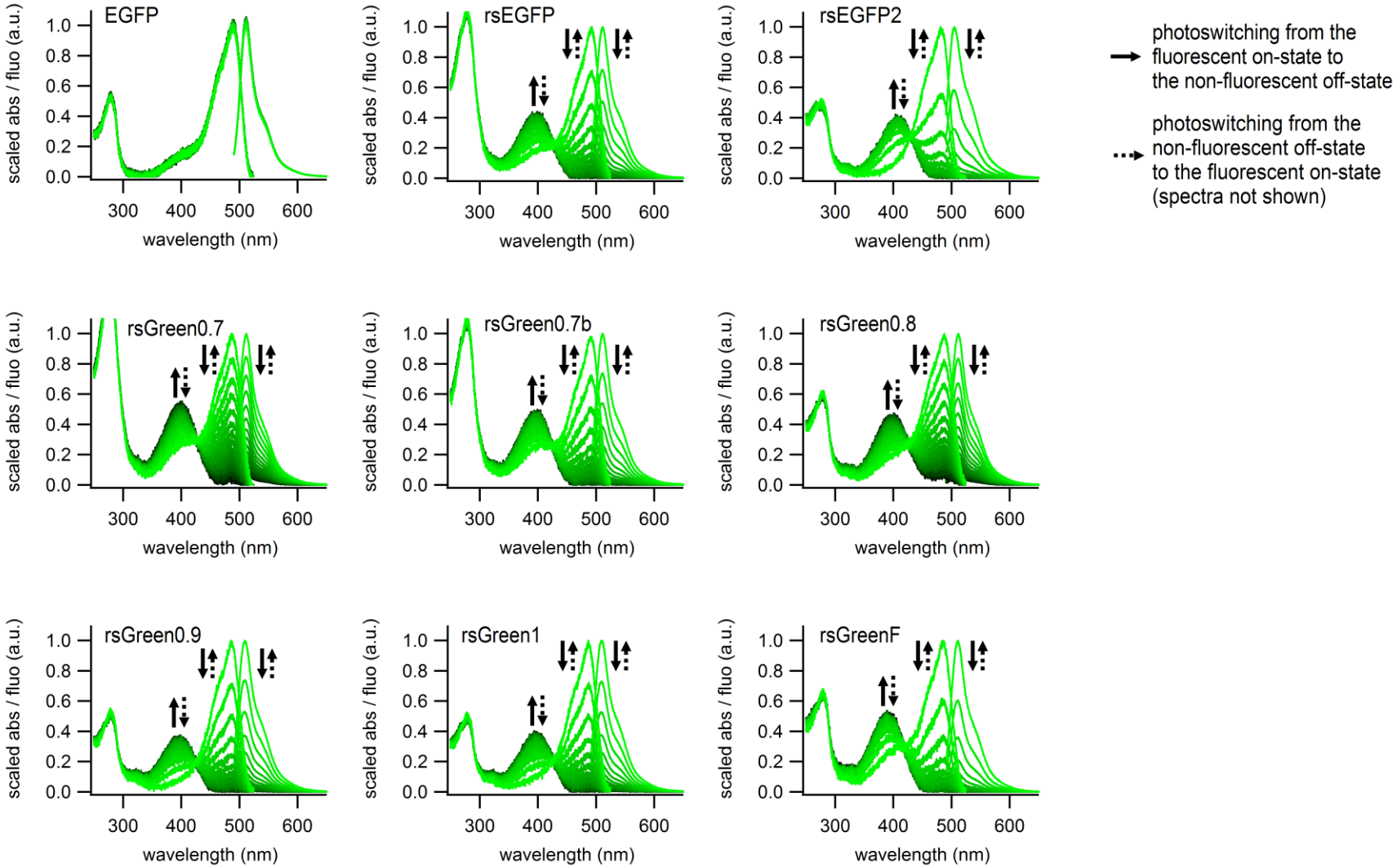

Figure S3: Absorbance and emission spectra (λ_{ex} = 473 nm) taken during the photoswitching of indicated FPs from the green on-state (green line) to the off-state (black line). During the reverse process, spectra recover to their initial state (not shown). All photoswitching measurements were performed with identical settings on purified protein solutions.

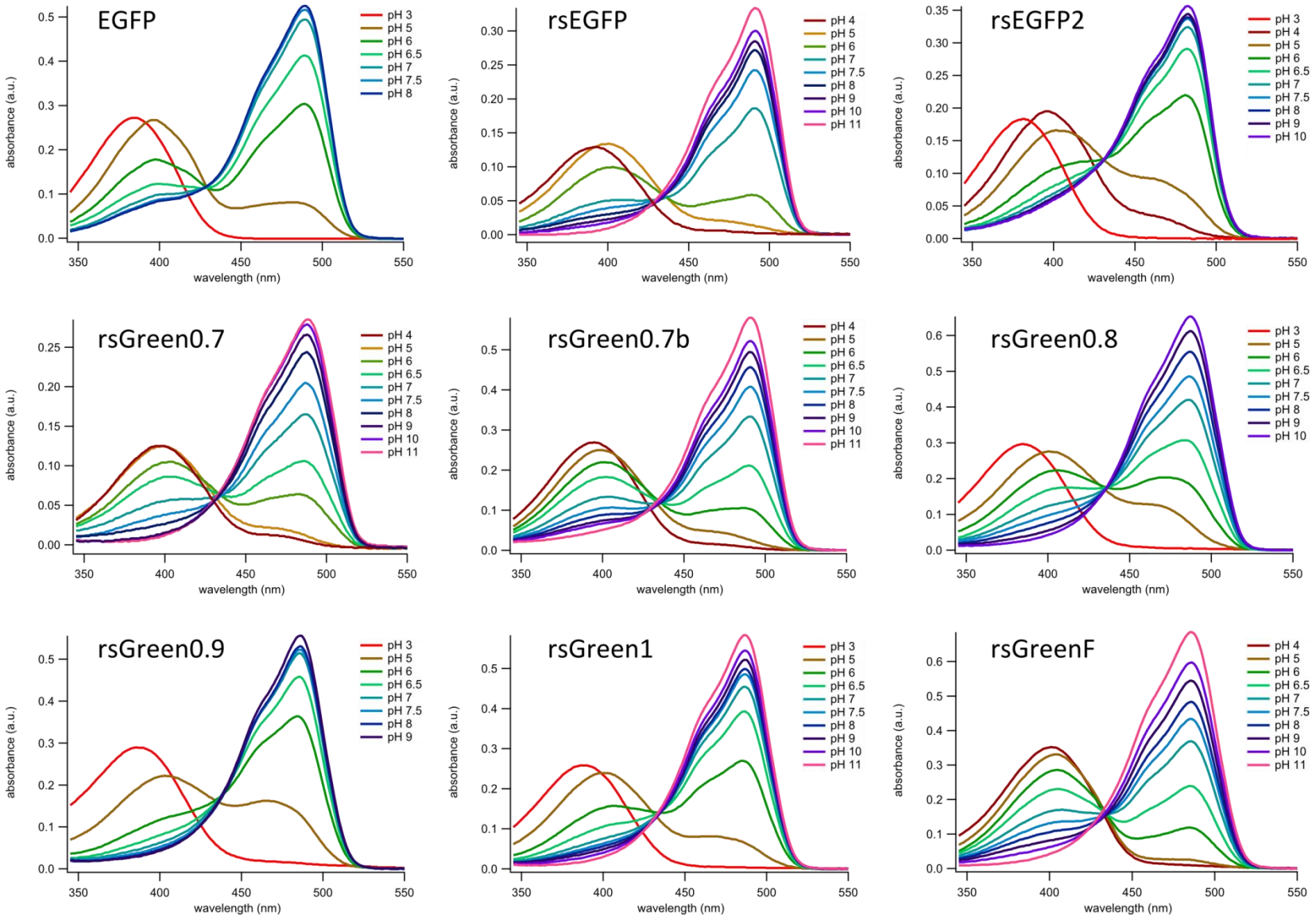

Figure S4: pH dependence of the absorbance spectra of the indicated FPs.

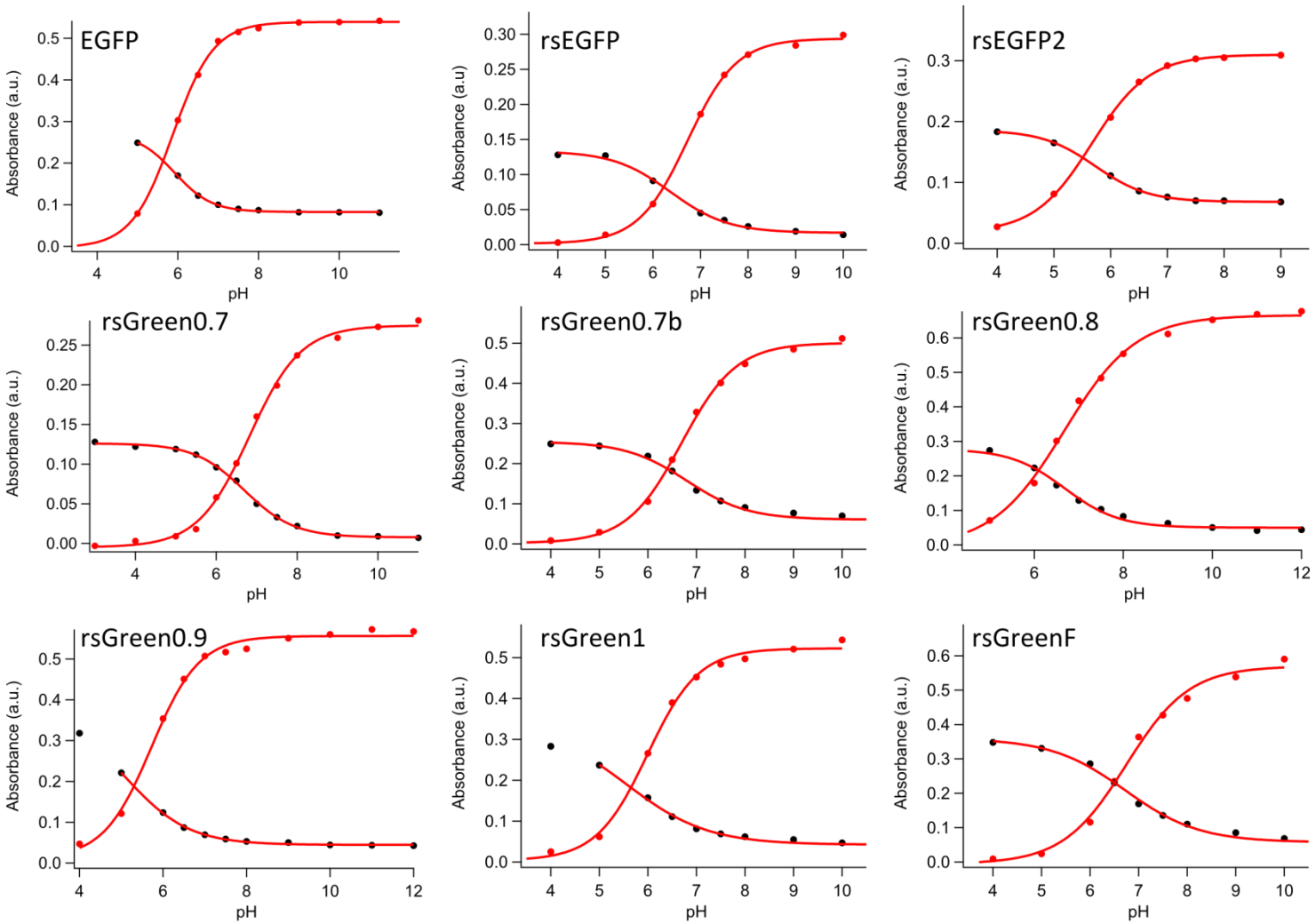

Figure S5: Maximal absorbance of the neutral and anionic peaks in function of pH. The inflection point of the sigmoidal fits corresponds to the pKa value of the chromophore.

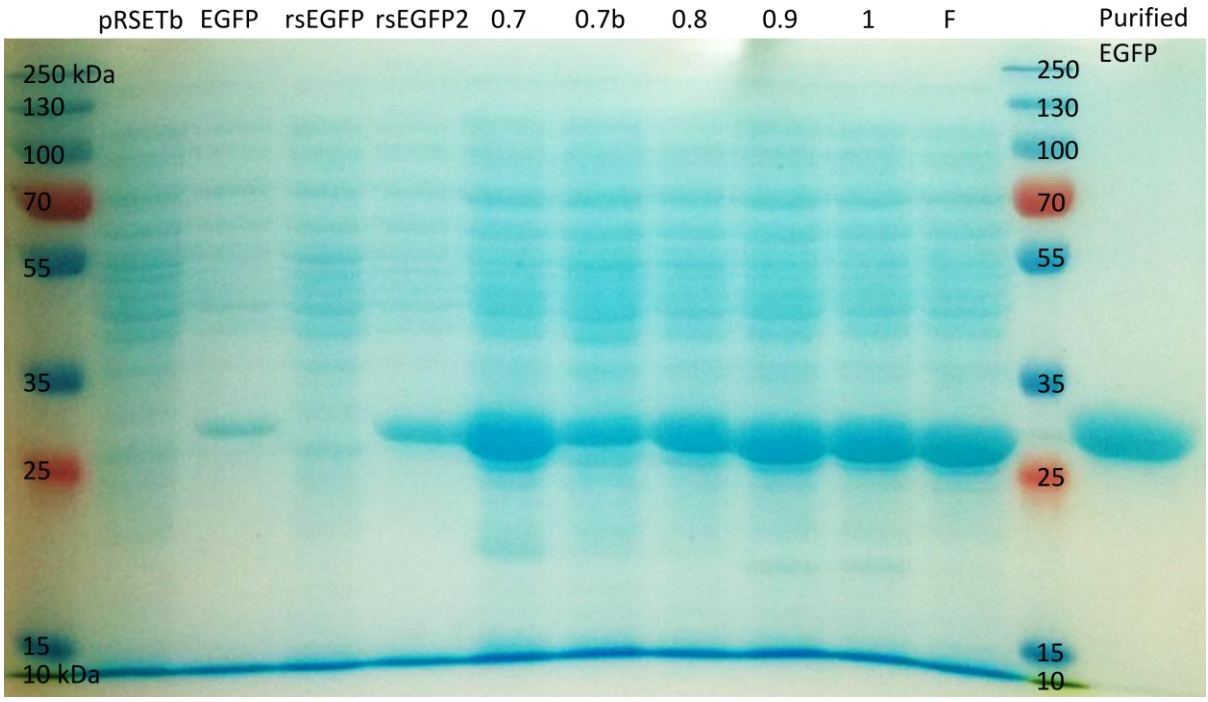

Figure S6: SDS-PAGE analysis of *E. coli* cultures expressing indicated FPs, grown at 37°C for 24 hours. All cultures show obvious expression of FPs, except for rsEGFP, indicating a hampered maturation efficiency and/or increased degradation.

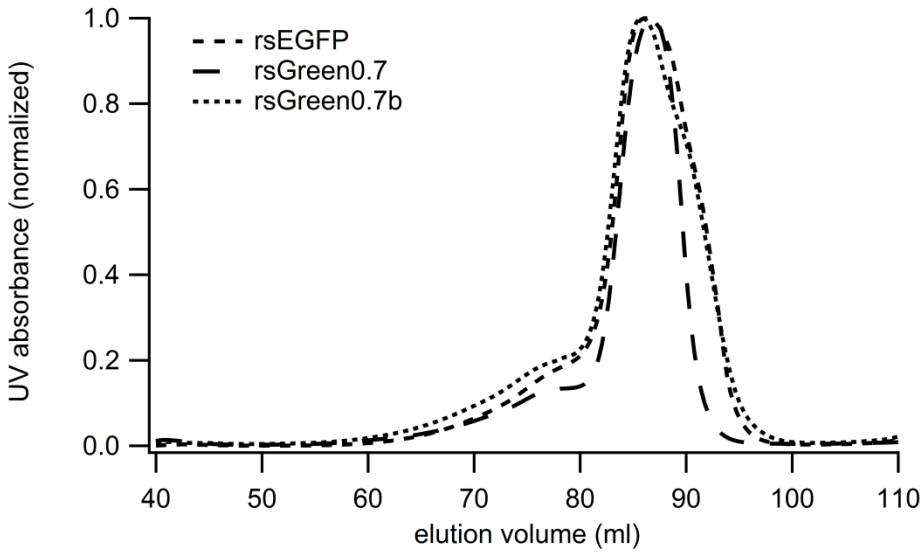

Figure S7: Size exclusion chromatography of rsEGFP, rsGreen0.7 and rsGreen0.7b, all containing a 29 AA purification tag. All FPs can be considered monomers evidenced by highly overlapping elution profiles and an estimated molecular mass <40 kDa well below an expected mass of >55 kDa for dimerizing FPs.

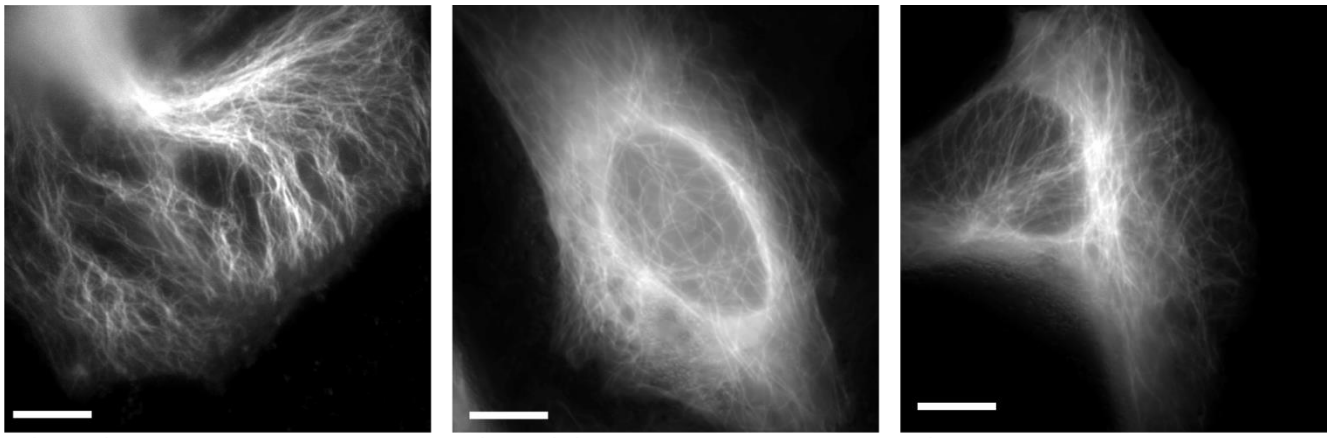

Figure S8: Wide-field microscopy images of rsGreen-tagged human α-tubulin in live HeLa cells. Images were taken by simultaneous illumination with 405 nm and 488 nm laserlight. Exposure times ranged from 200 - 1000 msec. Scale bars = 10 µm.

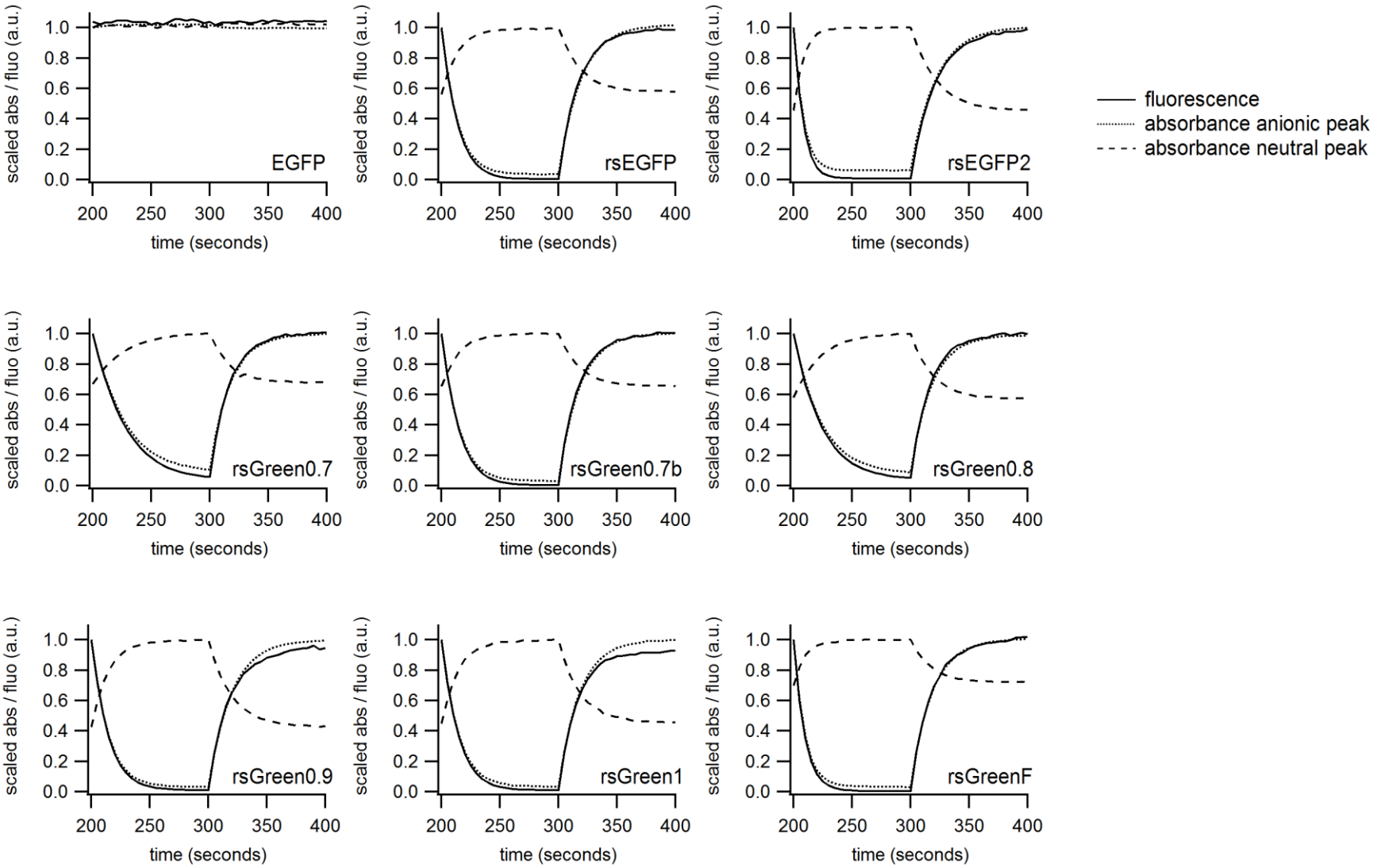

Figure S9: Photoswitching traces of the emission and absorption (neutral and anionic peak) maxima of indicated FPs, based on the data in figure S3. All photoswitching measurements were performed with identical settings on purified FP solutions.

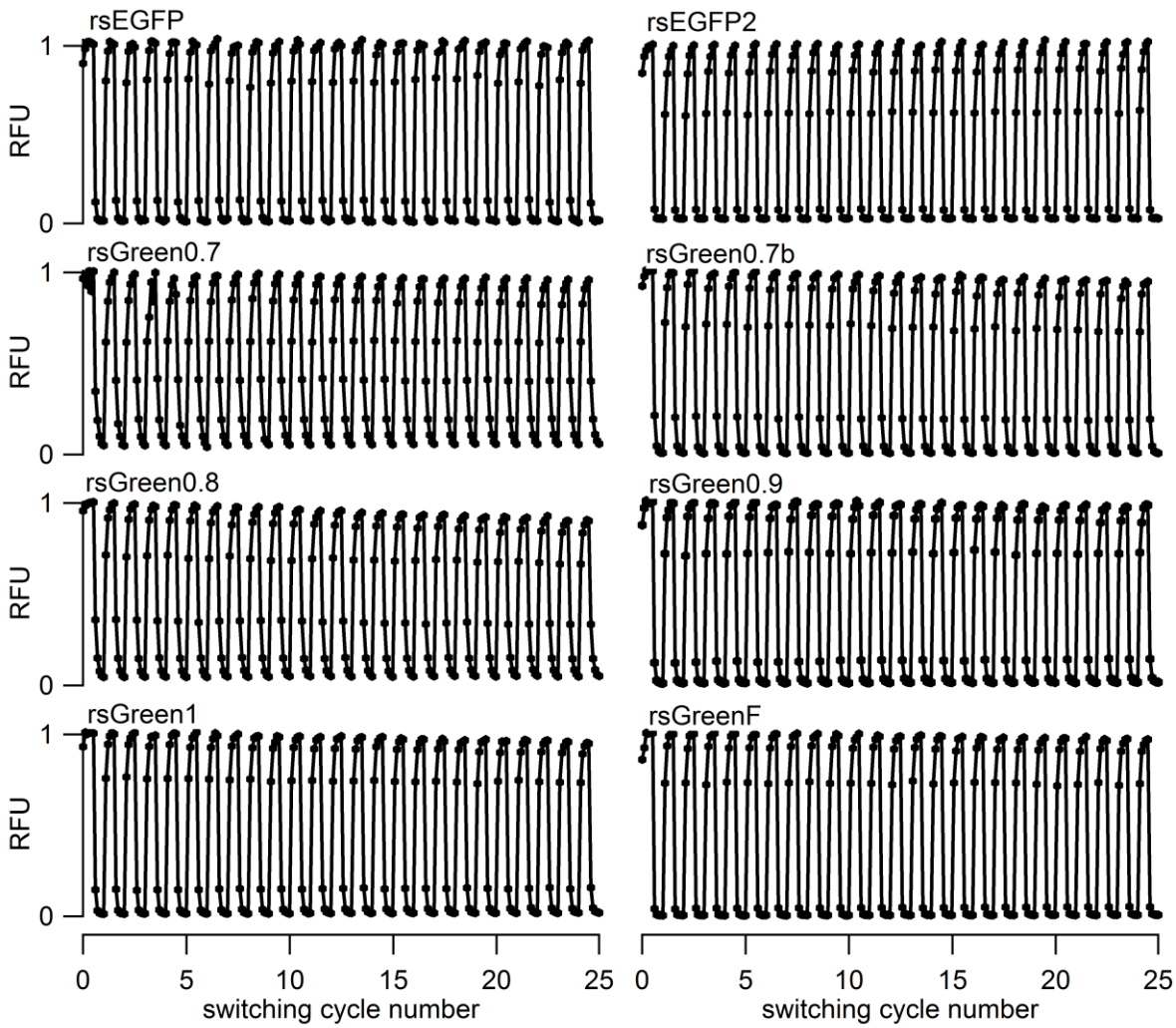

Figure S10: The initial 25 photoswitching cycles of indicated FPs measured in living HeLa cells on the Lumencor microscope. All samples were measured with identical photoswitching settings. Acquisition settings were adjusted for optimal use of the dynamic range of the setup.

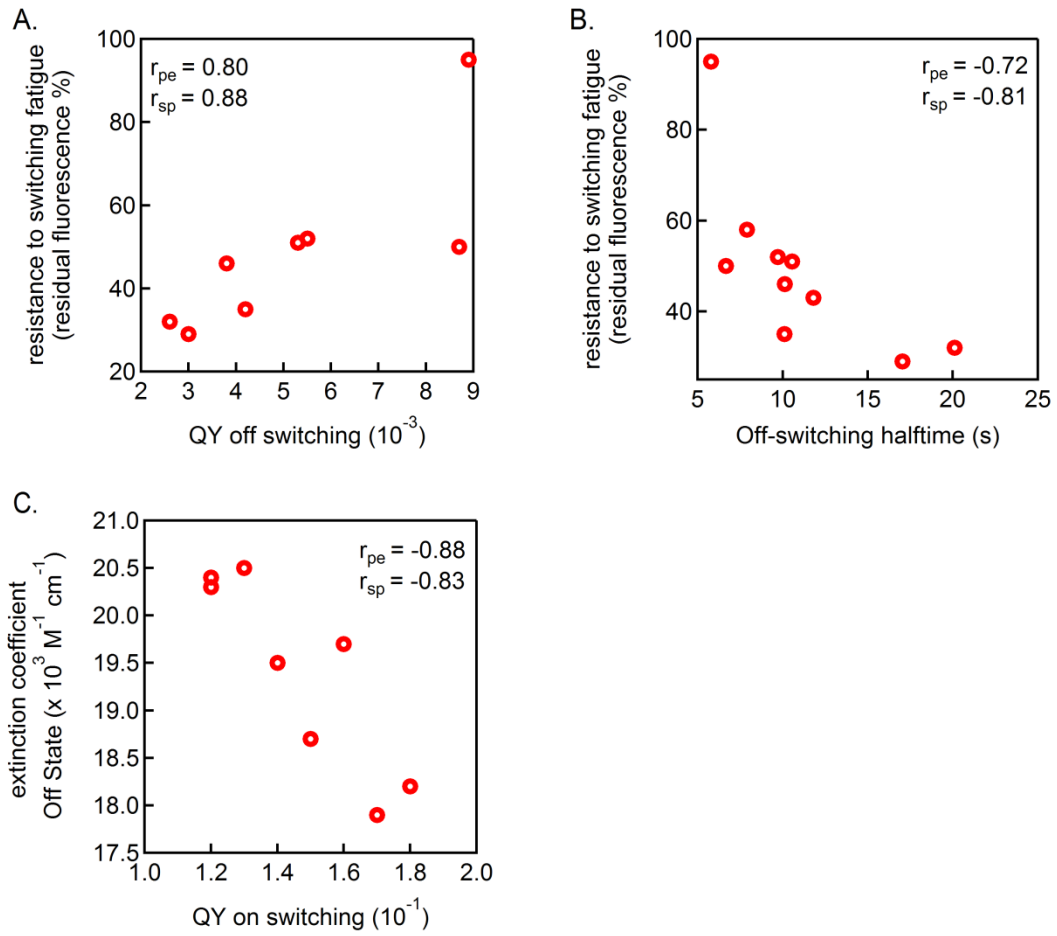

Figure S11: Significant correlations between the resistance to photoswitching fatigue and the efficiency of off-switching in terms of (A.) quantum yield (QY) and (B.) halftime, and (C.) between the off-state extinction coefficient and the on-switching efficiency. Photoswitching fatigue and off-switching halftime data for two additional rsGreen derivatives was added for the analysis. Pearsons correlation coefficient (r_{pe}) and Spearmans correlation coefficient (r_{sp}) were compared against their respective critical values for P = 0.05.

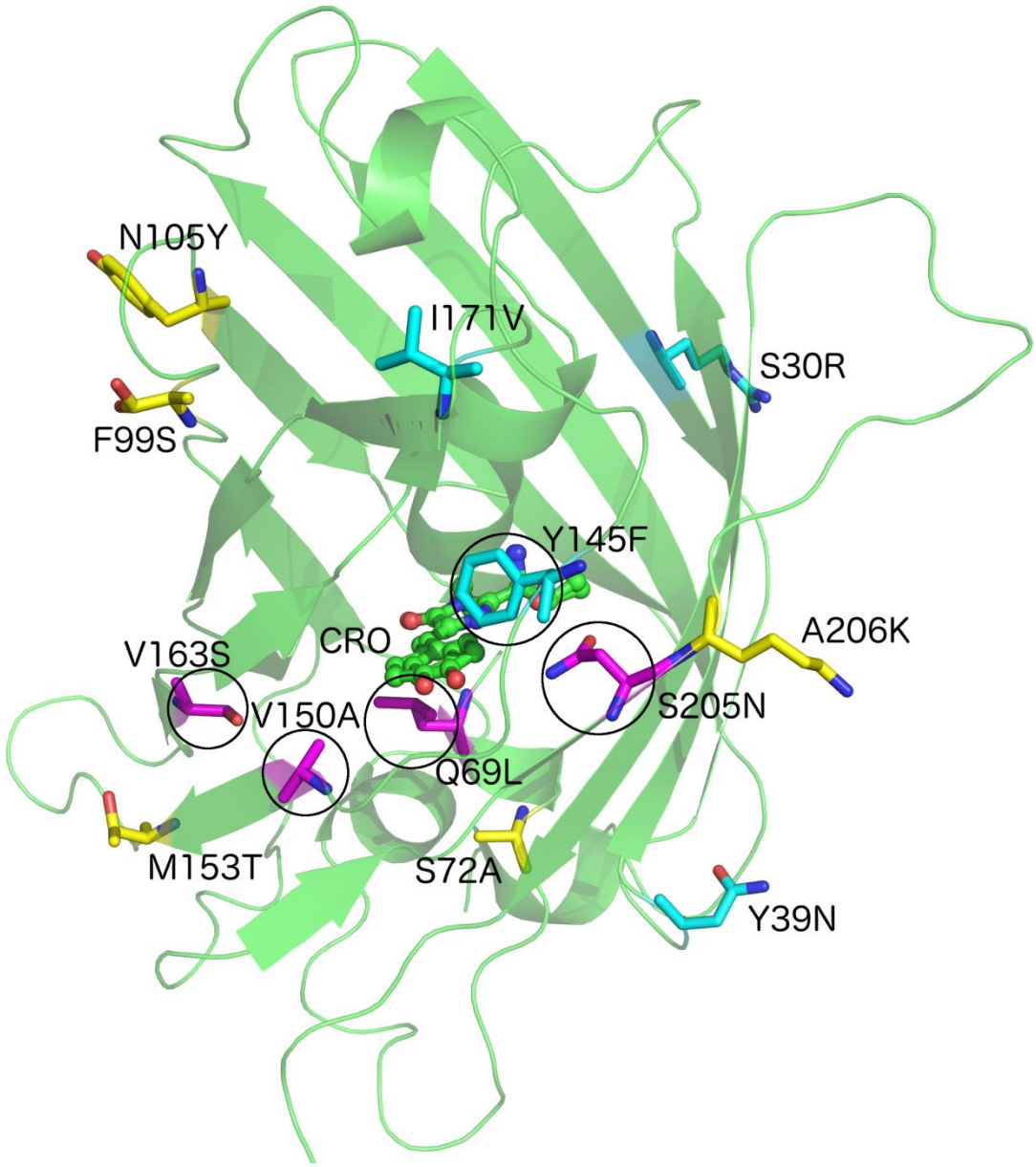

Figure S12: rsGreen0.7 mutations compared to EGFP. The β-can is depicted in green and bears the chromophore inside (ball and sticks). The rsEGFP mutations are depicted in magenta and the superfolder mutations in cyan. Other mutations are depicted in yellow. Mutations affecting the photoswitching behavior, indicated by the circles, are all situated around the chromophore.

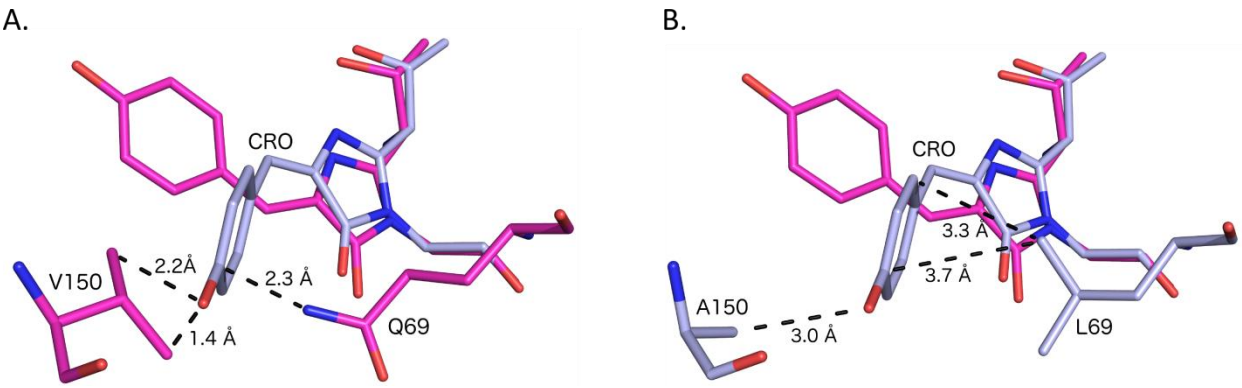

Figure S13: (A.) Unfavorable close contacts between the amino acids at position 69 and 150 in EGFP and the rsGreen0.7 off-state chromophore. EGFP is depicted in magenta (PDB ID: 4EUL), rsGreen0.7 in the off-state is depicted in gray. (B.) Due to the Q69L and the V150A mutations, enough space is created for the off-state chromophore.

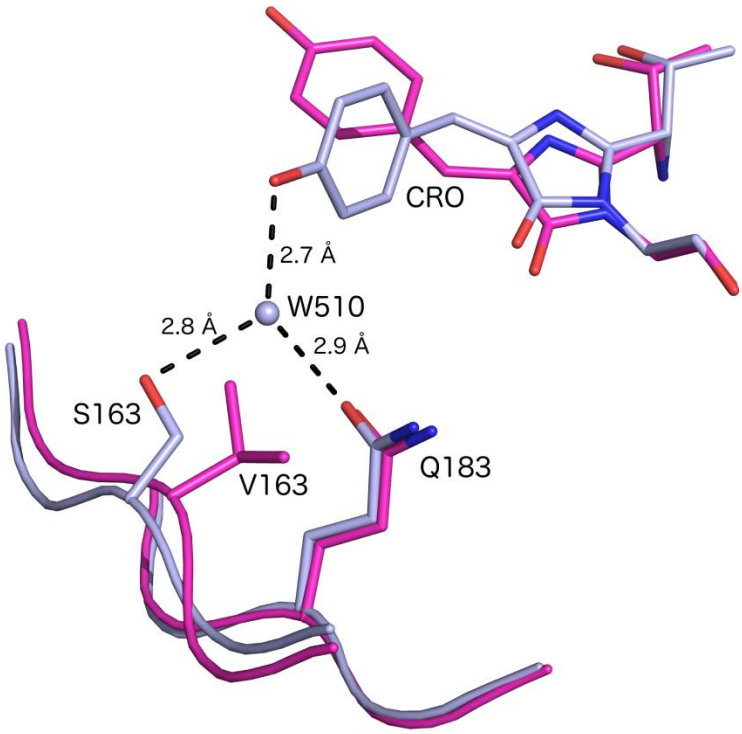

Figure S14: Hydrogen bonding network between the rsGreen0.7 off-state chromophore, water molecule 510 and residues 163 and 183 (grey). This network does not exist in the on-state of rsGreen0.7 or EGFP (PDB ID: 4EUL, magenta).

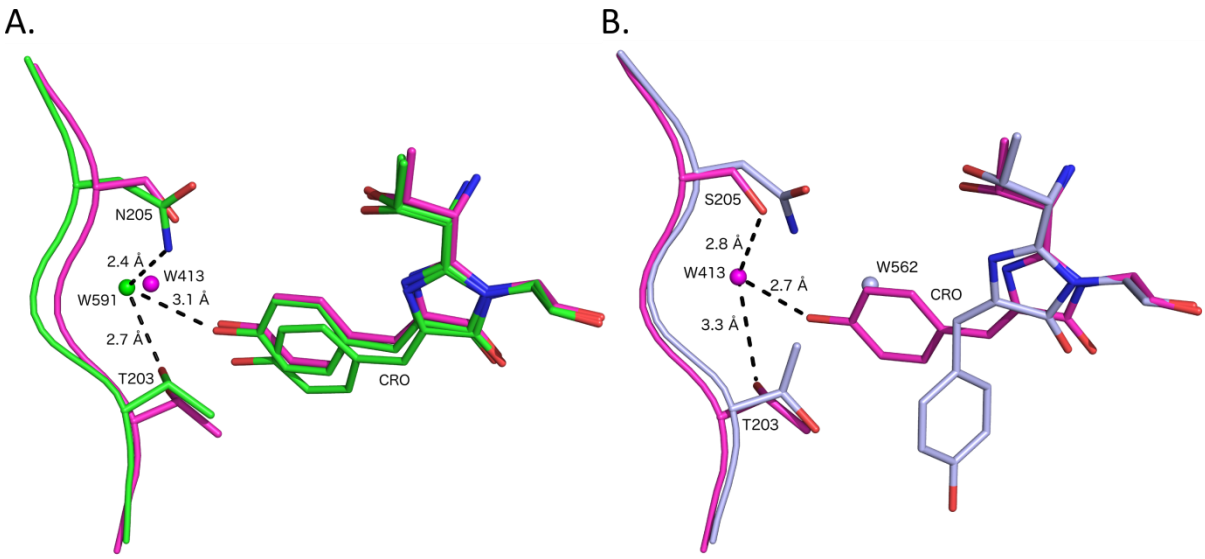

Figure S15: (A.) The S205N mutation is accompanied by a displacement of the rsGreen0.7 on-state protein backbone (green) compared to EGFP (PDB ID: 4EUL, magenta). The interactions between N205, T203, water molecule 591 and the chromophore are shown with dashes. (B.) In the off-state of rsGreen0.7 (gray), the protein backbone is superposable with the EGFP backbone. The dashes represent hydrogen bonding in EGFP, similar to the one shown in panel A.

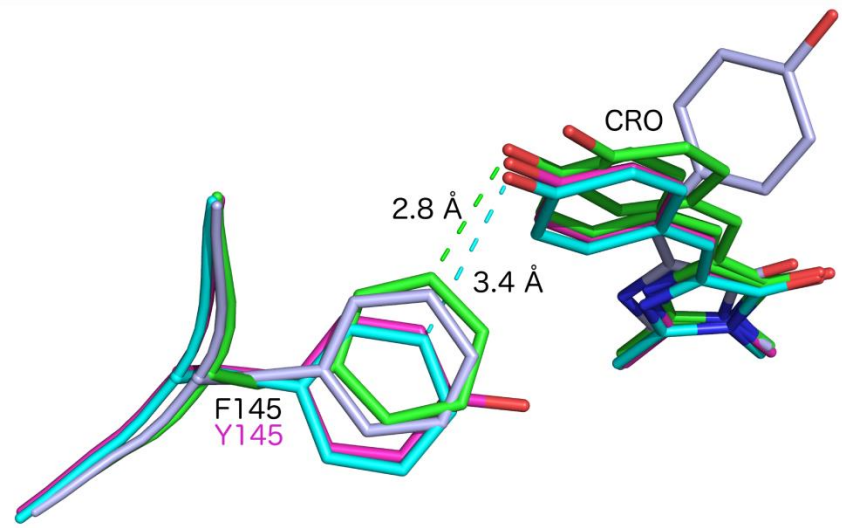

Figure S16: Structural comparison of EGFP (PDB ID: 4EUL, magenta) with tyrosine on position 145 and sfGFP (PDB ID 2B3P, cyan), rsGreen0.7 in the on- (green) and the off-state (gray), which all have phenylalanine on position 145.

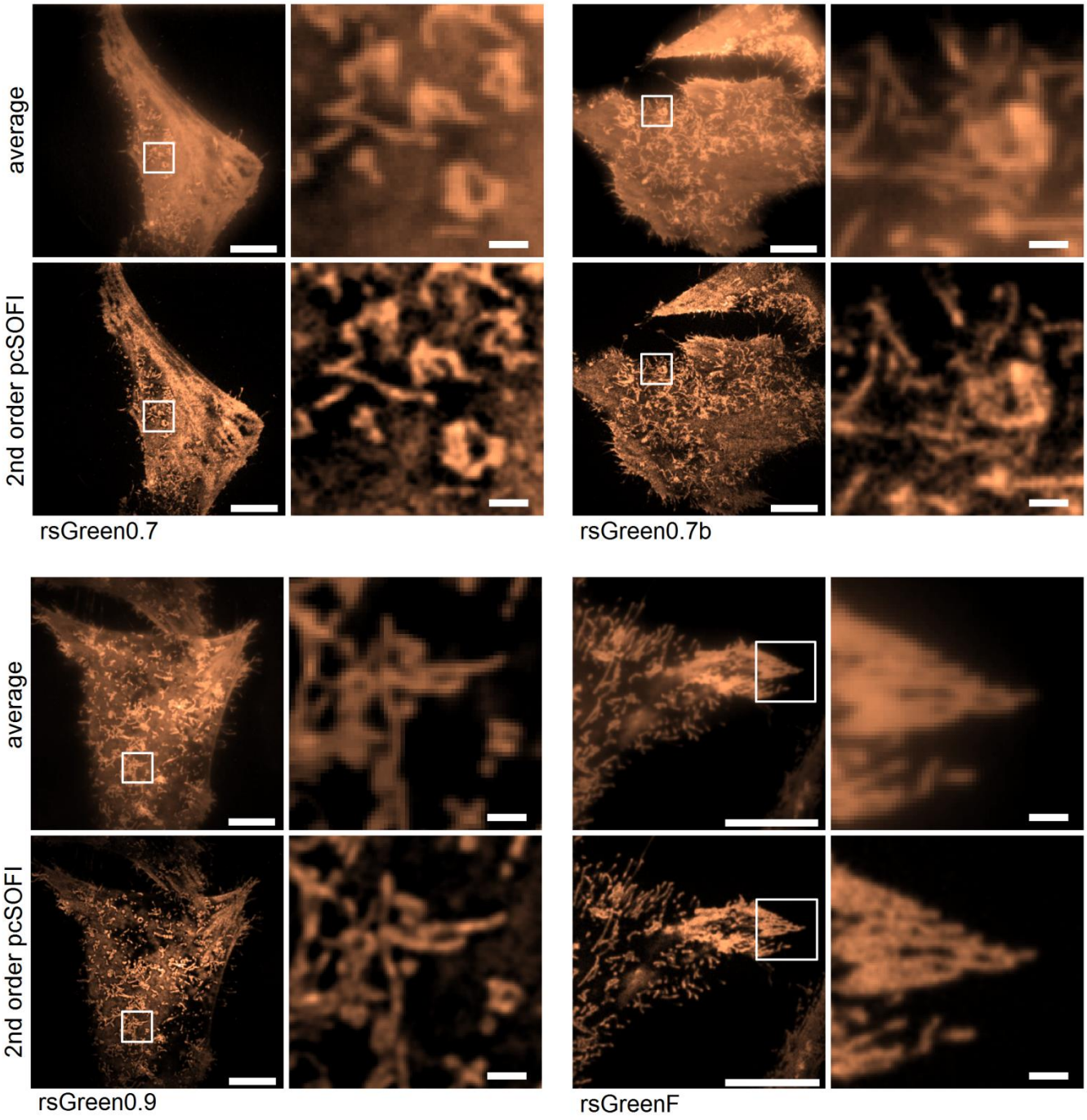

Figure S17: Sub-diffraction imaging with pcSOFI. Live Hela cells, transfected with pcDNA3::Lyn-rsGreen, imaged using TIRF mode illumination. Averaged widefield images and pcSOFI images including expansions of the boxed regions. Scale bars = 10 µm for the leftmost images and 1 µm for the expansions.

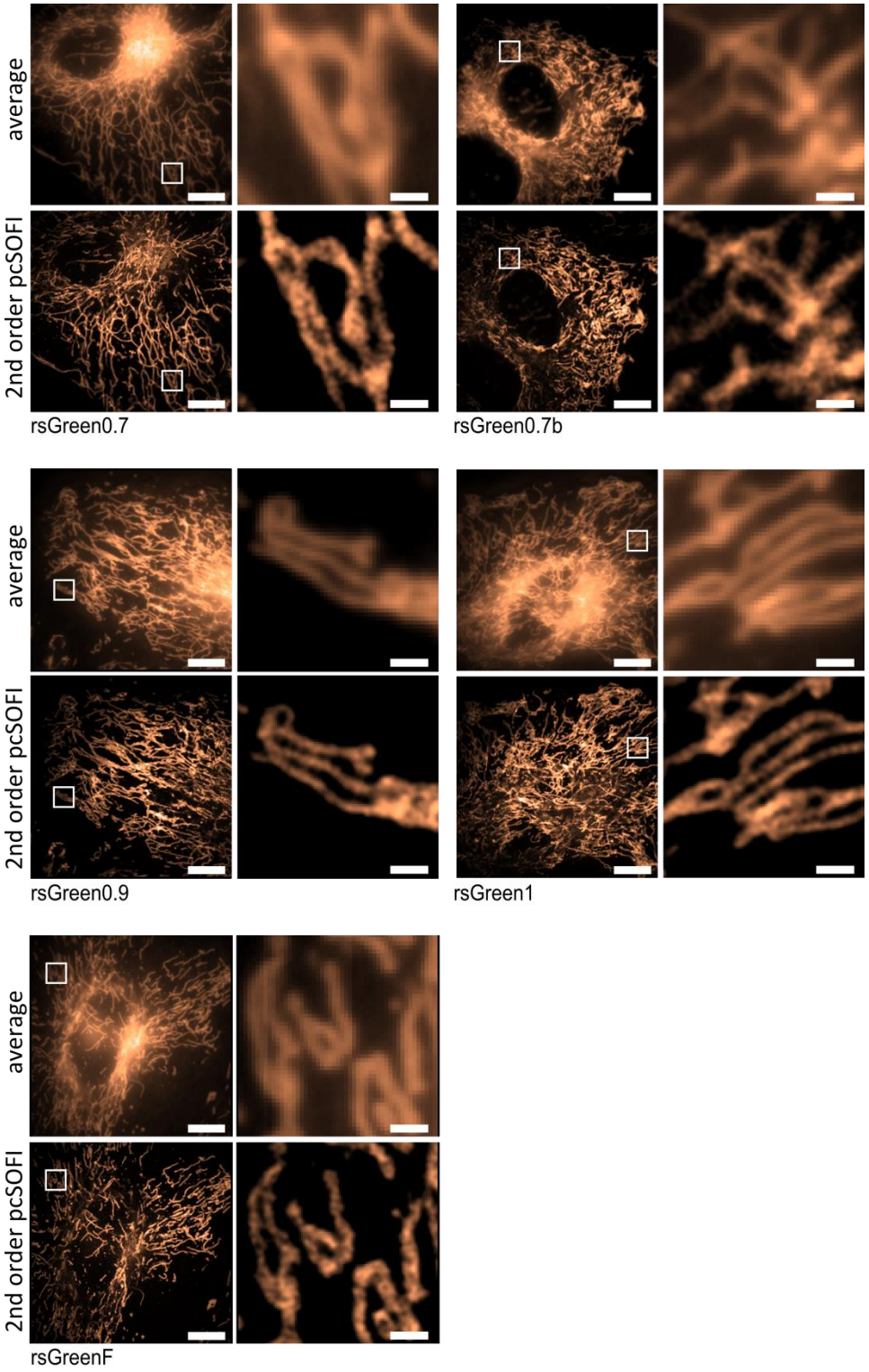

Figure S18: Sub-diffraction imaging with pcSOFI. Live Hela cells, transfected with pcDNA3::DAKAP-rsGreen, imaged using epi-mode illumination. Averaged widefield images and pcSOFI images including expansions of the boxed regions. Scale bars = 10 μm for the leftmost images and 1 μm for the expansions.

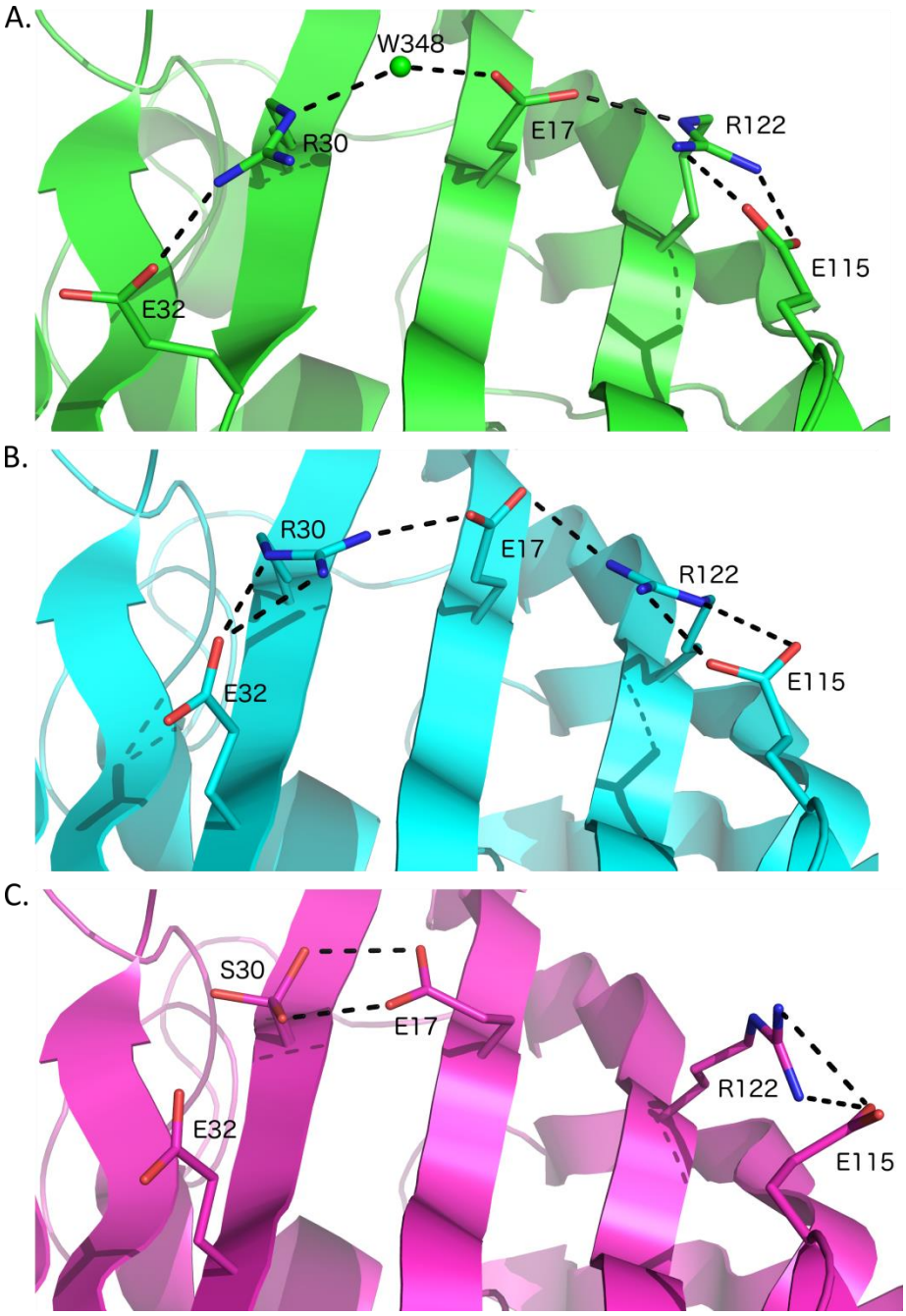

Figure S19: In rsGreen0.7 (A) and in sfGFP (PDB ID: 2B3P, B) a polar network between residue 32, 30, 17, 122 and 115 is established. In EGFP (PDB ID: 4EUL, C), where residue 30 is occupied by a serine, this network cannot be formed.

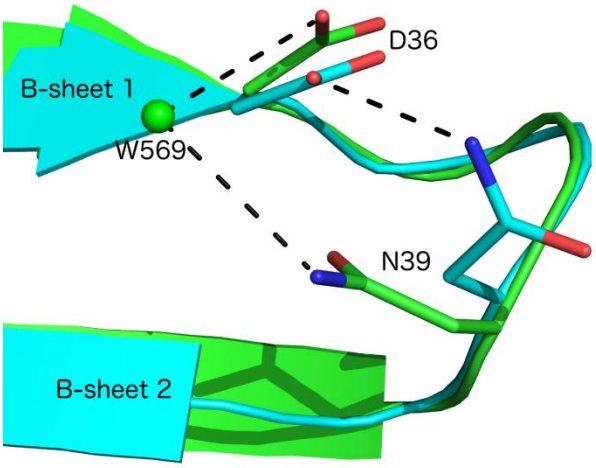

Figure S20: Hydrogen bonding of residues 36 and 39 for sfGFP (cyan) and rsGreen0.7 in the on-state (green). rsGreen0.7 requires the presence of water molecule 569 to provide hydrogen bonding interactions between residue 36 and 39.

SUPPORTING INFORMATION: REFERENCE SECTION

(1) Crameri, A.; Whitehorn, E. A.; Tate, E.; Stemmer, Wi. P. C. Improved Green Fluorescent Protein by Molecular Evolution Using DNA Shuffling. *Nat. Biotechnol.* **1996**, *14*, 315–319.

(2) Arpino, J. A. J.; Rizkallah, P. J.; Jones, D. D. Crystal Structure of Enhanced Green Fluorescent Protein to 1.35 Å Resolution Reveals Alternative Conformations for Glu222. *PLoS One* **2012**, *7*, e47132.

(3) Pédelacq, J.-D.; Cabantous, S.; Tran, T.; Terwilliger, T. C.; Waldo, G. S. Engineering and Characterization of a Superfolder Green Fluorescent Protein. *Nat. Biotechnol.* **2006**, *24*, 79–88.

(4) Xia, Y.; DiPrimio, N.; Keppel, T. R.; Vo, B.; Fraser, K.; Battaile, K. P.; Egan, C.; Bystroff, C.; Lovell, S.; Weis, D. D.; *et al.* The Designability of Protein Switches by Chemical Rescue of Structure: Mechanisms of Inactivation and Reactivation. *J. Am. Chem. Soc.* **2013**, *135*, 18840–18849.

(5) Gassner, N. C.; Baase, W. A.; Matthews, B. W. A Test of the "Jigsaw Puzzle" Model for Protein Folding by Multiple Methionine Substitutions within the Core of T4 Lysozyme. *Proc. Natl. Acad. Sci. U. S. A.* **1996**, *93*, 12155–12158.

(6) Fisher, A. C.; DeLisa, M. P. Laboratory Evolution of Fast-Folding Green Fluorescent Protein Using Secretory Pathway Quality Control. *PLoS One* **2008**, *3*, e2351.

(7) Erard, M.; Fredj, A.; Pasquier, H.; Beltolngar, D.-B.; Bousmah, Y.; Derrien, V.; Vincent, P.; Merola, F. Minimum Set of Mutations Needed to Optimize Cyan Fluorescent Proteins for Live Cell Imaging. *Mol. Biosyst.* **2013**, *9*, 258–267.

(8) Mizuno, H.; Dedecker, P.; Ando, R.; Fukano, T.; Hofkens, J.; Miyawaki, A. Higher Resolution in Localization Microscopy by Slower Switching of a Photochromic Protein. *Photochem. Photobiol. Sci.* **2010**, *9*, 239–248.

(9) Kabsch, W. Xds. *Acta Crystallogr. D. Biol. Crystallogr.* **2010**, *66*, 125–132.

(10) Adams, P. D.; Afonine, P. V; Bunkóczi, G.; Chen, V. B.; Davis, I. W.; Echols, N.; Headd, J. J.; Hung, L.-W.; Kapral, G. J.; Grosse-Kunstleve, R. W.; *et al.* PHENIX: A Comprehensive Python-Based System for Macromolecular Structure Solution. *Acta Crystallogr. D. Biol. Crystallogr.* **2010**, *66*, 213–221.

(11) McCoy, A. J.; Grosse-Kunstleve, R. W.; Adams, P. D.; Winn, M. D.; Storoni, L. C.; Read, R. J. Phaser Crystallographic Software. *J. Appl. Crystallogr.* **2007**, *40*, 658–674.

(12) Afonine, P. V; Grosse-Kunstleve, R. W.; Echols, N.; Headd, J. J.; Moriarty, N. W.; Mustyakimov, M.; Terwilliger, T. C.; Urzhumtsev, A.; Zwart, P. H.; Adams, P. D. Towards Automated Crystallographic Structure Refinement with Phenix.refine. *Acta Crystallogr. D. Biol. Crystallogr.* **2012**, *68*, 352–367.

(13) Emsley, P.; Lohkamp, B.; Scott, W. G.; Cowtan, K. Features and Development of Coot. *Acta Crystallogr. D. Biol. Crystallogr.* **2010**, *66*, 486–501.

(14) Moriarty, N. W.; Grosse-Kunstleve, R. W.; Adams, P. D. Electronic Ligand Builder and Optimization Workbench (eLBOW): A Tool for Ligand Coordinate and Restraint Generation. *Acta Crystallogr. D. Biol. Crystallogr.* **2009**, *65*, 1074–1080.

(15) Lam, A. J.; St-Pierre, F.; Gong, Y.; Marshall, J. D.; Cranfill, P. J.; Baird, M. A.; McKeown, M. R.; Wiedenmann, J.; Davidson, M. W.; Schnitzer, M. J.; *et al.* Improving FRET Dynamic Range with Bright Green and Red Fluorescent Proteins. *Nat. Methods* **2012**, *9*, 1005–1012.

(16) Cormack, B. P.; Valdivia, R. H.; Falkow, S. FACS-Optimized Mutants of the Green Fluorescent Protein (GFP). *Gene* **1996**, *173*, 33–38.

(17) Kremers, G.-J.; Goedhart, J.; van den Heuvel, D. J.; Gerritsen, H. C.; Gadella, T. W. J. Improved Green and Blue Fluorescent Proteins for Expression in Bacteria and Mammalian Cells. *Biochemistry* **2007**, *46*, 3775–3783.

(18) Tsien, R. Y. The Green Fluorescent Protein. *Annu. Rev. Biochem.* **1998**, *67*, 509–544.

(19) Shaner, N. C.; Steinbach, P. A.; Tsien, R. Y. A Guide to Choosing Fluorescent Proteins. *Nat. Methods* **2005**, *2*, 905–909.

(20) Teerawanichpan, P.; Hoffman, T.; Ashe, P.; Datla, R.; Selvaraj, G. Investigations of Combinations of Mutations in the Jellyfish Green Fluorescent Protein (GFP) That Afford Brighter Fluorescence, and Use of a Version (VisGreen) in Plant, Bacterial, and Animal Cells. *Biochim. Biophys. Acta* **2007**, *1770*, 1360–1368.

(21) Cubitt, A. B.; Woollenweber, L. A.; Heim, R. Understanding Structure-Function Relationships in the Aequorea Victoria Green Fluorescent Protein. *Methods Cell Biol.* **1999**, *58*, 19–30.

(22) Zapata-Hommer, O.; Griesbeck, O. Efficiently Folding and Circularly Permuted Variants of the Sapphire Mutant of GFP. *BMC Biotechnol.* **2003**, *3*, 5.

(23) Ito, Y.; Suzuki, M.; Husimi, Y. A Novel Mutant of Green Fluorescent Protein with Enhanced Sensitivity for Microanalysis at 488 Nm Excitation. *Biochem. Biophys. Res. Commun.* **1999**, *264*, 556–560.

(24) Kimata, Y.; Iwaki, M.; Lim, C. R.; Kohno, K. A Novel Mutation Which Enhances the Fluorescence of Green Fluorescent Protein at High Temperatures. *Biochem. Biophys. Res. Commun.* **1997**, *232*, 69–73.

(25) Baffour-Awuah, N. Y.; Fedeles, F.; Zimmer, M. Structural Features Responsible for GFPuv and S147P-GFP's Improved Fluorescence. *Chem. Phys.* **2005**, *310*, 25–31.

(26) Siemering, K. R.; Golbik, R.; Sever, R.; Haseloff, J. Mutations That Suppress the Thermosensitivity of Green Fluorescent Protein. *Curr. Biol.* **1996**, *6*, 1653–1663.

(27) Patterson, G. H.; Lippincott-Schwartz, J. A Photoactivatable GFP for Selective Photolabeling of Proteins and Cells. *Science* **2002**, *297*, 1873–1877.

(28) Chen, V. B.; Arendall, W. B.; Headd, J. J.; Keedy, D. a; Immormino, R. M.; Kapral, G. J.; Murray, L. W.; Richardson, J. S.; Richardson, D. C. MolProbity: All-Atom Structure Validation for Macromolecular Crystallography. *Acta Crystallogr. D. Biol. Crystallogr.* **2010**, *66*, 12–21.

(29) Wilmann, P. G.; Turcic, K.; Battad, J. M.; Wilce, M. C. J.; Devenish, R. J.; Prescott, M.; Rossjohn, J. The 1.7 A Crystal Structure of Dronpa: A Photoswitchable Green Fluorescent Protein. *J. Mol. Biol.* **2006**, *364*, 213–224.

(30) Andresen, M.; Stiel, A. C.; Trowitzsch, S.; Weber, G.; Eggeling, C.; Wahl, M. C.; Hell, S. W.; Jakobs, S. Structural Basis for Reversible Photoswitching in Dronpa. *Proc. Natl. Acad. Sci. U. S. A.* **2007**, *104*, 13005–13009.

(31) Moeyaert, B.; Nguyen Bich, N.; De Zitter, E.; Rocha, S.; Clays, K.; Mizuno, H.; Van Meervelt, L.; Hofkens, J.; Dedecker, P. Green-to-Red Photoconvertible Dronpa Mutant for Multimodal Super-Resolution Fluorescence Microscopy. *ACS Nano* **2014**, *8*, 1664–1673.

(32) Adam, V.; Lelimousin, M.; Boehme, S.; Desfonds, G.; Nienhaus, K.; Field, M. J.; Wiedenmann, J.; McSweeney, S.; Nienhaus, G. U.; Bourgeois, D. Structural Characterization of IrisFP, an Optical Highlighter Undergoing Multiple Photo-Induced Transformations. *Proc. Natl. Acad. Sci. U. S. A.* **2008**, *105*, 18343–18348.

(33) Pletnev, S.; Subach, F. V; Dauter, Z.; Wlodawer, A.; Verkhusha, V. V. A Structural Basis for Reversible Photoswitching of Absorbance Spectra in Red Fluorescent Protein rsTagRFP. *J. Mol. Biol.* **2012**, *417*, 144–151.

(34) Faro, A. R.; Carpentier, P.; Jonasson, G.; Pompidor, G.; Arcizet, D.; Demachy, I.; Bourgeois, D. Low-Temperature Chromophore Isomerization Reveals the Photoswitching Mechanism of the Fluorescent Protein Padron. *J. Am. Chem. Soc.* **2011**, *133*, 16362–16365.

(35) Brakemann, T.; Stiel, A. C.; Weber, G.; Andresen, M.; Testa, I.; Grotjohann, T.; Leutenegger, M.; Plessmann, U.; Urlaub, H.; Eggeling, C.; *et al.* A Reversibly Photoswitchable GFP-like Protein with Fluorescence Excitation Decoupled from Switching. *Nat. Biotechnol.* **2011**, *29*, 942–950.

(36) Andresen, M.; Wahl, M. C.; Stiel, A. C.; Gräter, F.; Schäfer, L. V; Trowitzsch, S.; Weber, G.; Eggeling, C.; Grubmüller, H.; Hell, S. W.; *et al.* Structure and Mechanism of the Reversible Photoswitch of a Fluorescent Protein. *Proc. Natl. Acad. Sci.* **2005**, *102*, 13070–13074.

(37) Henderson, J. N.; Ai, H.-W.; Campbell, R. E.; Remington, S. J. Structural Basis for Reversible Photobleaching of a Green Fluorescent Protein Homologue. *Proc. Natl. Acad. Sci. U. S. A.* **2007**, *104*, 6672–6677.